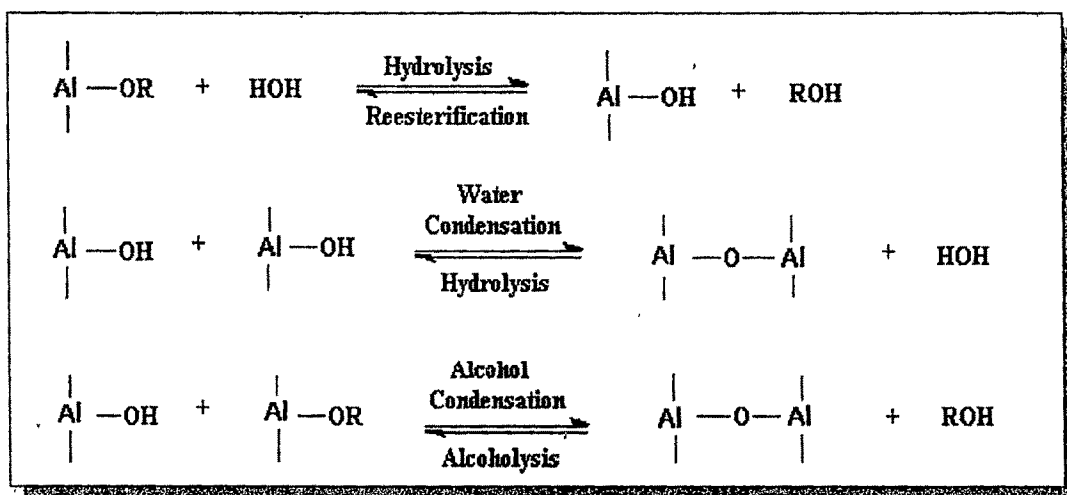


4. Studies on Alumina Support Prepared by Sol Gel Technique

In this Chapter the synthesis and characterization of alumina supports by two routes, namely, conventional Oil-drop (OD) and sol-gel (SG) are described. The inherent properties, like, surface area, pore volume, pore size distribution. Purity of crystalline phase, crystallinity, crystallite size, surface acidity and physical strength of the alumina samples obtained by these two methods have been compared. While the standard conditions of preparation (as elaborated in Chapter 3) have been adopted for OD method, a number of preparation parameters have been varied in the case of SG route.

4.1. Preparation of alumina by Sol – Gel Technique

Details of preparation methods are described in Chapter-3 and the major reactions involved during SG process are described in Scheme 4.1.



Scheme 4.1 Equations showing the sol – gel process

To recapitulate, during the hydrolysis reaction, the addition of water, replaces secondary butoxide groups (OBu) of Aluminum Secondary Butoxide (ASB) with hydroxyl groups (OH). Subsequent condensation reactions involving the Al – OH groups produce Al-O-Al bonds plus water or alcohol as the by-products. Normally, condensation commences before hydrolysis is complete. However, conditions such as, pH, H₂O/Alkoxide molar ratio (R), and catalyst can force completion of hydrolysis before condensation begins (1). In presence of n-butanol as solvent/ homogenizing agent, the hydrolysis is facilitated due to the miscibility of the alkoxide and water

(2). As the number of Al – O – Al bonds increases, the individual units are bridged and jointly aggregate in the sol. When the sol particles aggregate, or inter-knit into a network, a gel is formed. Upon drying, trapped volatiles (water, alcohol, etc.) are driven off and the network shrinks as further condensation can occur. It should be emphasized, however, that the addition of solvents and certain reaction conditions might promote esterification and depolymerization reactions according to the reverse of equations.

Thus a series of reactions take place leading to the formation of the gel, whose structure is determined by the preparation conditions/parameters.

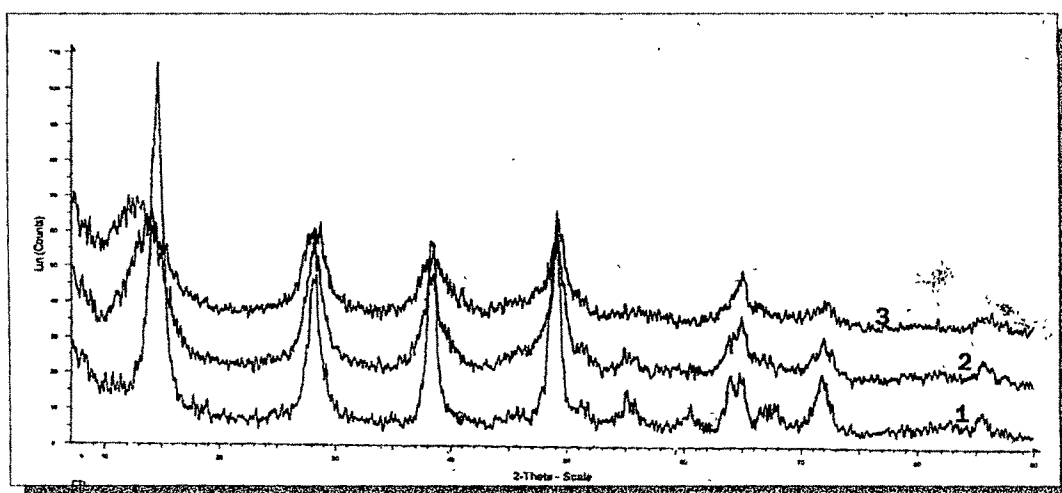


Figure 4.1: X – ray diffractograms of alumina precursors prepared by (1) Oil drop technique (2) Acid catalyzed sol – gel technique (3) Base catalyzed sol – gel technique

In the current study alumina and alumina supported Pt-Sn catalysts were prepared using the SG technique. The effect of various parameters viz. nature of hydrolysant (protic and aprotic), hydrolysis level "h" (molar ratio of water to alkoxide); acid and base catalysis of the hydrolysis step were investigated. The materials were characterized through various techniques viz. N₂ adsorption, SEM, XRD, IR and Thermogravimetry.

4.2. Characterization of alumina precursors

XRD studies indicate the presence of pseudoboehmite phase in all the alumina precursors obtained, irrespective of the preparation method or variations in preparation parameters. Fig. 4.1 show diffractograms of precursors through Oil drop technique and two typical precursors, ASG and BSG, representing preparations under acidic (pH = 3) and basic (pH = 9) conditions, through sol – gel. All major d-lines at 2θ values $\sim 14, 28, 49, 55, 64, 65$ and 72 , **(3)** characteristic of pseudoboehmite phase, are clearly observed in oil drop and ASG precursors while the BSG precursor is highly amorphous.

Oil drop precursor displays better crystallinity and higher crystallite size as compared to ASG precursor.

Formation of boehmite phase in the case of SG samples is in line with the preparation conditions adopted in the present work, wherein hydrolysis of ASB was carried out at 80°C , followed by its condensation at 90°C . Yoldas et al **(4)** report that at temperatures less than 80°C yield bayerite phase with relatively small crystallite size whereas temperatures greater than 80°C result in pseudoboehmite. Gomez et al **(5)** has also reported the formation of amorphous hydroxides with immediate transformation to pseudoboehmite at hydrolysis temperatures greater than 80°C .

Characterization of the precursors by thermal analysis confirms the presence of pseudo boehmite, along with some small amounts of bayerite in some cases. (Table 4.1 and Fig. 4.2)

In the thermogravimetric studies pure commercial bayerite and boehmite were taken as references. Bayerite is an alpha trihydroxide of aluminium and it rapidly transforms completely to η - phase at 280°C in air saturated with moisture **(6)**. Commercial pseudoboehmite transforms into gamma alumina at 470°C . These transformation temperatures are close to those reported for the respective alumina precursors.

Table 4.1 Phase Transformations in alumina precursors through Thermal Analysis

Sr. No.	Sample	Transition Temperatures (°C)		Boehmite content (%)	Bayerite content (%)	Weight Loss (%) (RT - 600°C)
1.	Bayerite	280.44 (η - phase)	-	0.00	100.00	31.46
2.	Pseudoboehmite (Vista)	-	470.75 (γ - phase)	100.00	0.00	19.31
3.	Alumina precursor from oil drop route	266.40 (η - phase)	429.63 (γ - phase)	65.02	0.79	18.24
4.	Alumina precursor from acid catalyzed SG	-	454.59 (γ - phase)	67.50	0.00	23.92
5.	Alumina precursor from base catalyzed SG	262.09 (η phase)	457.60 (γ phase)	79.98	0.57	20.00

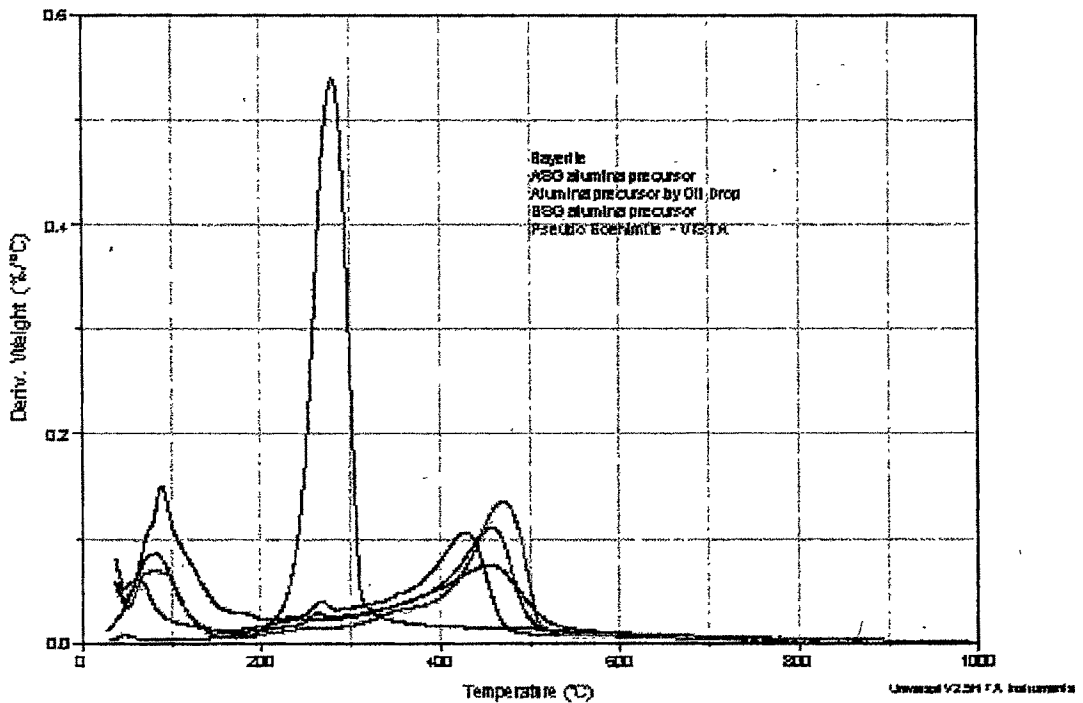


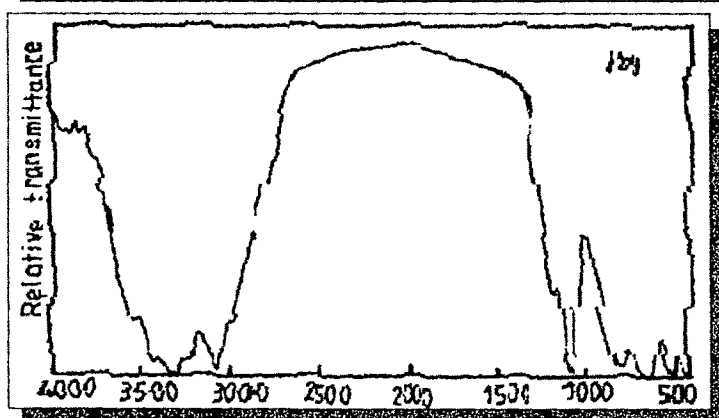
Figure 4.2 Thermogravimetric studies of alumina precursors prepared by different routes

It is observed that the alumina precursors obtained through base catalyzed sol gel and the oil drop technique have a small amount of bayerite, which is expected since both have their origins in alkaline media prevalent during preparation. For the sol gel alumina prepared in acidic medium bayerite is absent.

For the transformation of crystalline boehmite to γ -alumina the expected weight loss is 15% (7). However, in all the alumina precursors prepared in this work and also for a commercial boehmite sample, weight losses are around 18-24 %. Physically adsorbed water and solvent and organic moieties account for the extra weight losses. Table 4.2 gives the weight loss in stages, wherein such losses are observed up to 200°C. Losses in the range 200-600 °C are attributed to the phase transformation of pseudoboehmite to γ -alumina, which is as per expectations.

Table 4.2
Weight loss of dried alumina prepared from different routes

Sample	Temperature range	
	0 °C – 200 °C (Wt %)	200°C – 600°C (Wt %)
Acid catalyzed SG alumina precursor	10.62	13.88
Base catalyzed SG alumina precursor	5.95	14.50
Alumina precursor from oil drop route	4.98	14.74
Pseudoboehmite – VISTA	3.877	14.55



IR spectra of the precursor samples (Fig 4.2a) also confirm the presence of pseudoboehmite phase.

Figure 4.2a: IR Spectra of alumina precursor

4.3. Effect of Sol-Gel Preparation Parameters

4.3.1. Effect of pH

The two main processes involved in the preparation of alumina through the sol – gel route are hydrolysis of the ASB and the condensation of the resultant sol into a gel. Under acidic conditions, the hydrolysis rates increase while condensation proceeds faster in the presence of base catalysts **(8)**.

In the hydrolysis step, regardless of pH, hydrolysis occurs by the nucleophilic attack of the oxygen contained in water on the aluminium atom of the ASB **(9)**.

Condensation occurs by either an alcohol producing or a water-producing reaction. Engelhardt and his team **(10)** showed that a typical sequence of condensation products is monomer → dimer → linear trimer → cyclic trimer → cyclic tetramer → higher order rings. This sequence of condensation requires both depolymerization (ring opening) and the availability of monomers, which are in solution equilibrium with the oligomeric species and/or are generated by depolymerization.

The rate of these ring opening polymerizations and monomer addition reactions is dependent upon the environmental pH. In polymerizations below pH 2, the condensation rates are proportional to the $[H^+]$ ion concentration. The developing gel networks are composed of exceedingly small primary particles.

It is observed that between pH 2 and pH 6 condensation rates are proportional to $[OH^-]$ ion concentrations **(11)**. Condensation preferentially occurs between more highly condensed species and those less highly condensed and somewhat neutral. This suggests that the rate of dimerization is low, however, once dimers form, they react preferentially with monomers to form trimers, which in turn react with monomers to form tetramers. Cyclization occurs because of the proximity of the chain ends and the substantial depletion of the monomer population. Further growth occurs by

addition of lower molecular weight species to more highly condensed species and aggregation of the condensed species to form chains and networks.

Above pH 7, polymerization occurs in the same manner as in the pH 2 - 6 range. However, in this pH range, condensed species are ionized and therefore, mutually repulsive. Growth occurs primarily through the addition of monomers to the more highly condensed particles rather than by particle aggregation. Due to the greater solubility of alumina and the greater size dependence of solubility above pH 7, particles grow in size and decrease in number as highly soluble small particles dissolve and reprecipitate on larger, less soluble particles. Growth stops when the difference in solubility between the smallest and largest particles becomes indistinguishable. This process is referred to as Ostwald ripening. Particle size is therefore, mainly temperature dependent, in that higher temperatures produce larger particles. Additionally, in this pH range, the growth rate depends upon the particle size distribution

Base catalyzed gels are thought to be composed of branched open chains of particles. Work of Poelz **(12)** suggests that a higher pH leads to larger particles and pores with a more homogenous pore size distribution.

At higher pH due to increased availability of hydroxyl ions the charge on the colloidal particle is greater so that the particles grow to larger diameters hence a decrease in surface area. In the condensation step, the three major forces play a vital role in controlling the gelation process. They are (1) Van der Waals forces (2) Electrostatic forces (3) chemical (specifically, hydrogen) bonding.

The first two are of importance. The electrostatic force can be changed more readily by altering the pH. Such pH changes affect the surface potential and hence Van der Waals forces. Each particle then agglomerates via Van der Waals forces of attraction to form a 3D network **(13)**.

Acid Catalyzed



Yield primarily linear or randomly branched polymer

Base Catalyzed



Yield highly branched clusters

Figure 4.2b

In short, the growth of the gel network is controlled by the pH and accordingly surface area and pore structure of the alumina precursor/alumina are determined. A schematic representation of the gel network formed under two extreme pH conditions, acidic and basic, is given in Fig. 4.2b.

Gomez et al (5), report that the surface area of alumina samples prepared (by SG) calcined at 600°C increases with pH from 120m²/g at pH 3 to about 240m²/g in the range of pH 6-9 with a sharp drop at pH 10 due to the use of NaOH (for pH 10) resulting

from formation of Sodium aluminate. They attribute the low surface area at pH 3 to high branching during the condensation stage. Balakrishnan and Gonzalez (14), however report results to the contrary with no noteworthy change in surface area (typically 900m²/g) or pore diameter (typically 4nm) for samples dried at 120°C for 24h, on varying the pH from 0.8 to 10.3. However these authors achieved pH 10.3 with NH₄OH and not NaOH.

Effect pH on textural properties of alumina/catalysts, as observed in the current studies is described in Table.4.3. While the samples at pH 7 and 10 correspond to alumina, the one at pH 3 is Pt-Sn/Al₂O₃ catalyst, wherein < 1 wt% Pt and Sn as their chlorides were incorporated. Keeping in mind the small quantities of these metallic constituents, it is expected that they would not influence the textural properties as much as the pH, adjusted by the addition of aqueous HCl.

Table 4.3 Effect of pH on textural properties of SG Alumina

Sample code	Ph	Surface Area (m ² /g)	Pore Volume (ml/g)	Mean pore radius (Å)	Hysteresis Loop Form
PH3	3	250	0.65	35	Type I or II
PH7	7	216	0.74	69	Type II
PH9	9	379	1.75	92	Type IV or V
PH10	10	220	0.83	75	Type IV Or V

As expected, surface area, pore volume and mean pore radius increase with pH with the sample prepared at pH 9 showing maximum values. Under basic pH, excepting for the alumina sample prepared at pH 9, the other samples yielded similar surface area (215-220 m²/g) and pore volume (~ 0.74 – 0.83 ml/g). The results are consistent with those obtained by Gomez et al (5). However the surface areas of the alumina samples prepared in this study were observed to be much higher than those reported by Gomez et al (5) A drastic reduction in surface area at higher pH as observed by Gomez et.al is not evidenced in the present work since the total water content are 10 moles and it dilutes overall availability of the hydroxyls.

4.3.2. Evaluation of textural properties of sol-gel alumina

The qualitative aspects of the twofold description of texture of porous solids by Salmones et al (15) was used for classifying the alumina samples prepared in the current study. This classification is based on the modeling of a porous solid as an assemblage of directly or alternately linked sites (antrae or cavities) and bonds (capillaries or passages) to form a connected 3-D network. The authors show that size segregation (the probability of sites and bonds of the largest size tending to form regions of relatively large pores while elements of the smallest size constituting domains of small expanse) increases as overlap between the size distribution of sites and bonds increases. This size segregation influences the processes of capillary condensation and evaporation based on which porous materials can be classified into one of 5 types. The shape of the hysteresis loop (*HLF – Hysteresis loop form*) is a typical signature of the kind of relative size of sites and bonds forming the porous system. This classification enables differentiation of the structure of the porous material between a truly connected network or a collection of independent pores such as free spaces between parallel plates. Besides this, information regarding the mechanical rigidity of the material is also obtained. The method also outlines the limitations in determination of pore size distribution of samples wherein percolative processes in the desorption isotherm interfere with ascertainment

of large pores, while the tensile strength effect (sudden closure of the HLF) affecting determination of small pores.

On applying the description above to the alumina samples in the current study, it is observed that the morphology and rigidity of the samples change with pH. At pH 3 and pH 7 (without addition of NH_4OH), the HLF (Fig.4.3) was of type II with incomplete pore blockage during desorption of the adsorbate and sloping adsorption and desorption isotherms, consistent with size disparity between the elements of the porous system and a non-rigid structure that contracts/expands during capillary condensation/evaporation. At higher pH 9 or 10 a type IV or V HLF is evident, indicative of consolidated unifoliate elements with no percolative or pore blocking effects.

4.3.3. Effect of solvents

Diluents or solvents are used for two reasons. While both aid in the control of hydrolysis, the solvent helps homogenize the mixture, in addition. Although the solvent, on account of formation or absence of "H" bridge formation with the nucleophile $(\text{OH})_2\text{-Al-O}^-$, in the case of protic and aprotic solvents respectively, is expected to affect the relative rates of hydrolysis and condensation (which are the key to final textural properties of the material) Gomez et al (5) report in their studies that texture and structure of the final calcined product appear to be totally independent of these polar effects resulting in surface areas typically in the range 180-220 m^2/g , in spite of the use of solvents with varied polarity, such as ethanol, trichloromethane, carbon tetrachloride and acetonitrile.

Hence in the present work this aspect was not studied and use was made of normal butanol, (the parent alcohol in ASB) as the solvent. Other reasons for its choice were good solubility of ASB besides miscibility with the hydrolysant solution, which in this study was a mixture of water and Iso propylalcohol (IPA).

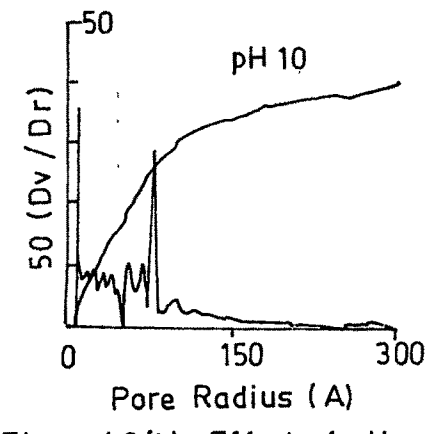
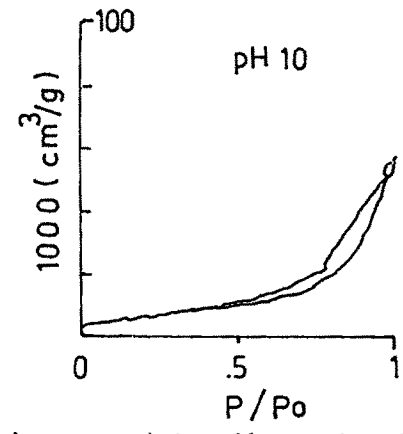
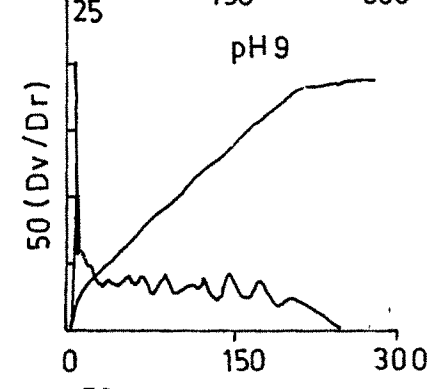
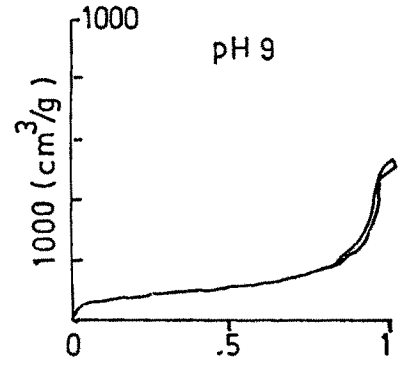
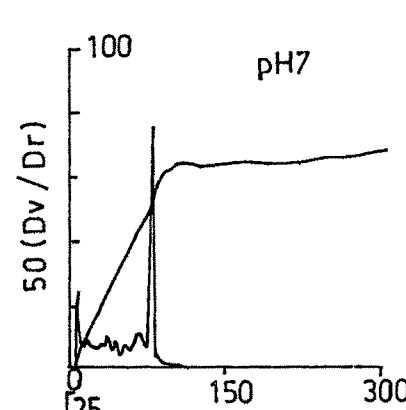
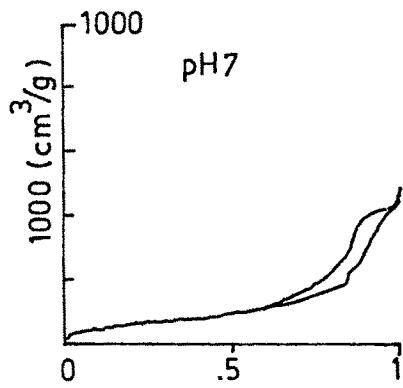
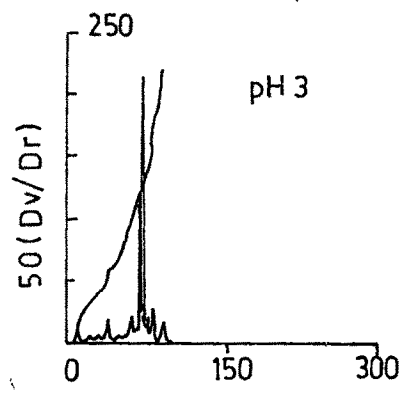
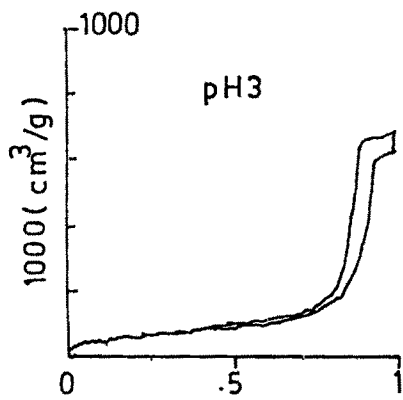


Figure 4.3(a): Effect of pH on textural properties: Hysteresis Loop Form

Figure 4.3(b): Effect of pH on textural properties: Pore size distribution curves

4.3.4. Water to Diluent ratio

It is widely reported in published literature on SG that the rate of hydrolysis is one of the crucial parameters in determining the textural properties of the final support. This is controlled by dilution of both ASB as well as the hydrolysant; water, with an alcohol or organic solvent. Since hydrolysis is associated with a nucleophilic substitution mechanism it is interesting to see the effects that are produced during gelation as a function of the polarity of the solvent used. The protic polar solvents (H_2O) have a tendency to decrease the condensation rate by deactivation of the nucleophile $(OH)_2-Al-O$ by hydrogen bridge interaction. On the contrary, aprotic polar solvents (IPA) do not deactivate the nucleophile because they have no hydrogen atoms capable of forming bridges (13).

The hydrolysant (water) was diluted with IPA in the above studies; however rate of addition of hydrolysant was maintained constant for all experiments at 1 ml/min.

Table 4.4 Effect of hydrolysis ratio on textural properties

Sample Code	Base to Alkoxide ratio	H ₂ O:IPA (v/v)	Surface Area (m ² /g)	Pore Volume (ml/g)	Mean pore radius (Å)	HLF
IPA 0	200	Water only	283	0.55	39	Type I or II
IPA 0.5	133	1:0.5	287	0.73	51	Type IV
IPA 1	100	1:1	379	1.75	92	Type IV or V

In the present study, IPA was used to diluent water. Reason for choice of IPA was formation of a single homogeneous phase of the water-IPA-normal butanol mixture. Three dilutions as volumetric ratios H₂O:IPA=0, 0.5, 1 corresponding to molar ratios α , 8.5 and 4.3 respectively were studied. However since another parameter, the hydrolysis level "h" also changed inadvertently, independent effect of this parameter could not be established. Samples with a volumetric ration of 1:1 (water:IPA) were observed to yield the best results in terms of high surface area, pore volume and mean pore radius, morphology and mechanical property (Table 4.4) and on the basis of these results the ratio of water to diluent was maintained at 1:1 (vol/vol) for all further studies.

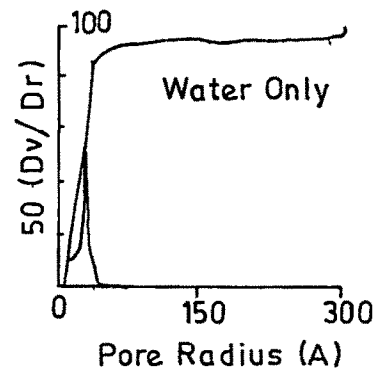
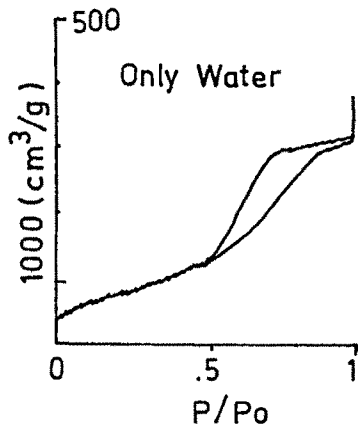
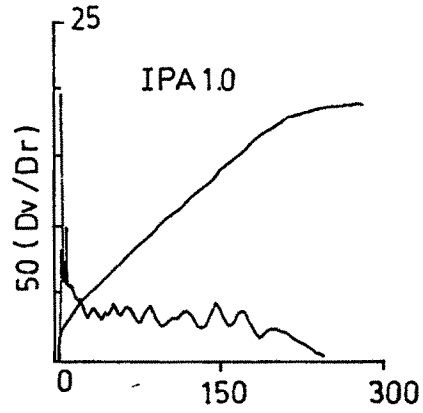
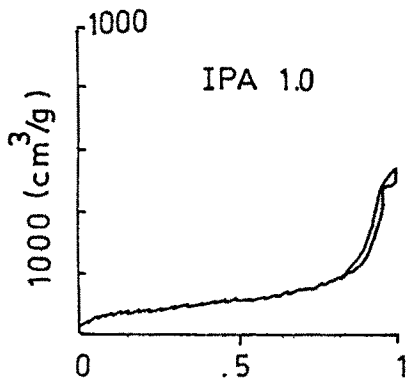
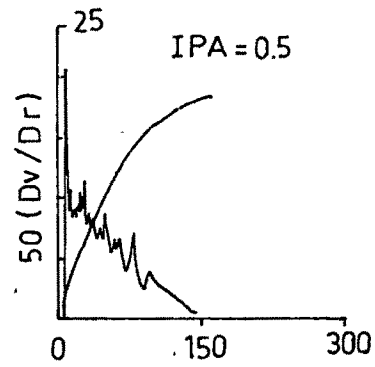
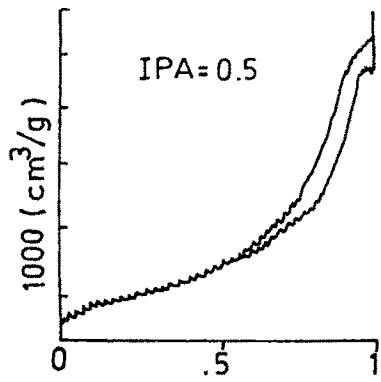


Figure 4.4(a): Effect of hydrolysis ratio on textural properties : Hysteresis Loop Form

Figure 4.4 (b): Effect of hydrolysis ratio on textural properties : Pore size distribution curves

4.3.5. Effect of hydrolysis level

Hydrolysis level "h" is generally referred to as the mole ratio of the hydrolysant (Water) to that of the Aluminium precursor (Aluminium Secondary Butoxide). Stoichiometric molar ratio for the reaction is 3. In the current work H₂O, ASB molar ratio (100, 133, and 200) was studied. Values of "h" below 100 were not studied, because study of Yoldas (4) show that excess water is required for densification of the alumina material. Study of Salmones, (16) also shows that use of less water results in soft unconsolidated material. The relevant hysteresis loop forms are given in Fig. (4.4). Effect of variations in hydrolysis levels on the textural properties are presented in Table 4.4

The use of "h" = 100 results in alumina with a Type IV or V hysteresis loop form Both the adsorption (ABC – Ascending boundary curve) as well as desorption (DBC - Descending boundary curve) curves are sloping, i.e. free from percolative effects. Pore blocking effect during desorption is absent as is evident from the absence of the horizontal initial plateau of the DBC. This is indicative of a pore structure with more or less uniform sized elements (antrae as well as channels). The sample appears to be a resultant of a process of almost complete consolidation with fair amount of mechanical rigidity.

Increasing the hydrolysis level "h" from 100 to 200 results in a decrease in surface area to the extent of about 25% as well as pore volume to an extent of 68%. The mean pore diameter is also seen to decrease to an extent of 57%. The hysteresis loop form changes progressively to Type IV and then to Type I or II, indicative of progressive transition to larger size disparity between the antrae and the passages (elements) of the porous structure. The initial region of the DBC is sloping indicating a contracting non-rigid structure with incomplete pore blocking effects. At "h"=200 percolative evaporation in the DBC curve are evident (as seen by a sudden drop in the DBC curve after the initial gradual slope) which is consistent with this type of structure. However a sharp end point of the DBC is not observed.

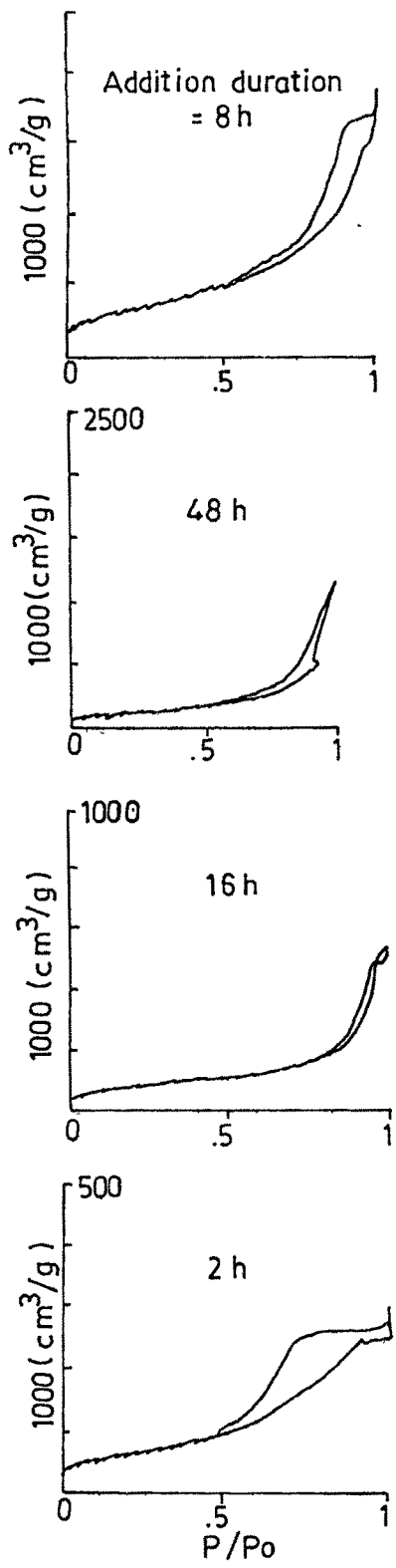


Figure 4.5(a): Effect of hydrolysant addition duration on textural properties: Hysteresis Loop Form

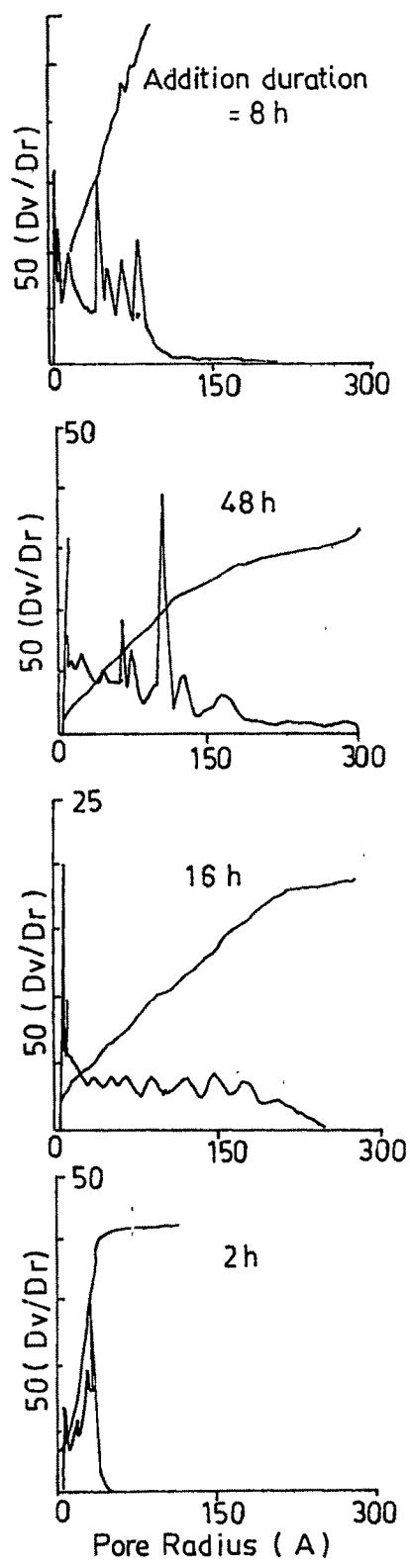


Figure 4.5(b): Effect of hydrolysant addition duration on textural properties: Pore size distribution

The value of "h" used in all further work in the present studies was 100. Observations in the current work in this aspect are in line with those reported in literature.

Studies of Balakrishnan et al (**14**), show that surface area (samples dried at 120°C 24 h) decreases (from 1137 to 352 m²/g), mesoporosity increases at the expense of microporosity, pore diameter increases from 3 to 9 nm with increase in "h" from 1.5 to 15. It is however important to note that the authors report a decrease in the surface area to the tune of 48% with attendant increase in pore diameter from 5 to 9 nm on calcinations of the samples in air at 500°C for 2 h. The advantage of high surface area and pore volumes obtained for silica prepared by sol-gel method are offset by this decrement in the case of alumina samples.

4.3.6. Effect of rate of hydrolysant addition

Balakrishnan et al (**14**) recommends a slow rate of addition since uncontrolled hydrolysis results in phase segregation and consequent loss of homogeneity. This parameter is expected to affect both the rate of hydrolysis and the relative form of condensation / oxolation either through alcohol condensation or water condensation or olation depending on the concentration of M-OH species in the reaction medium. A fast addition is expected to result in a larger concentration of M-OH with greater possibility of oxolation through condensation of water or olation. This could also result in phase segregation.

In the present studies this parameter was studied to a minimal extent, durations of 4-6h and 48 h were studied. Effect of very slow rate of addition of hydrolysant solution, over duration of 48 h yielded a sample with a BET specific surface area of 266 m²/g with attendant specific pore volume 0.76 ml/g (Refer Table 4.5). The isotherm was type V as per classification of Salmones et al (**15**) with a very narrow hysteresis loop and sloping ABC and

DBC, (Fig. 4.5), indicative of unifoliate structural elements with no evidence of percolative effects, as expected of this type of structure. The pore size distribution was wide showing a combination of micro, meso and macropores with the micropores predominating. In the present studies this parameter was maintained at 1ml/min resulting in a typical hydrolysis time of 6 hours because such samples were observed to give a predominantly mesoporous distribution which is desirable for the target reaction (paraffins dehydrogenation) under study.

4.4. Effect of Ageing of sol

Effect of aging was also studied by changing the duration of aging post-hydrolysis from 2 to 16 h. Slow hydrolysant addition rate over duration of 48 hours was also studied. During this period concomitant aging along with hydrolysis is likely to occur, with a greater probability for oxolation through alcohol condensation rather than water condensation or olation. Results are given in Table 4.5

The following inferences can be drawn from the above results:

Aging over duration of 16 h results in good surface area and pore volume with almost unimodal mesoporous distribution, pore radius in the range of 103-106 Å. The hysteresis loop form conforms to type IV with sloping ABC and DBC and a narrow hysteresis loop indicative of relatively small difference between the elements (of the pore system) and a consolidated porous structure. This kind of structure is desirable for the target reaction (paraffins dehydrogenation) under consideration.

Table 4.5 Effect of hydrolysant addition rate on textural properties

Sample	Duration of hydrolysant addition (h)	Surface Area (m ² /g)	Pore Volume (ml/g)	Pore radius (Å) Max Contribution	HLF
AS-0	0	226	0.84	Microporous	Type III
AS-2	2	226	0.84	30-35	Type II
AS-8	6	234	0.49	50	Type II
AS-16	16	379	1.75	103-106	Type IV
AS-48	48	266	0.76	Broad	Type V

Decreasing the aging (condensation time) to 2h results in a hysteresis loop for of Type I or II with decrease in both surface area as well as pore volume. Pore size

distribution exhibits maximum contribution from pores of lower radii 30 to 35 Å or even microporosity in certain cases. The hysteresis loop form is indicative of gross disparity between the size of adjacent elements of the pore system, with attendant percolative behaviour in the DBC.

Increasing the aging duration to 48 h results in decrease in specific surface area and specific pore volume (to the same extent as low aging time) but the hysteresis loop form indicates a consolidated structure with unifoliate elements, type V. The pore size distribution is broad covering the entire range from micro to macropores.

Of the above textures that obtained with 16 h aging duration is the most desirable for the target reaction; hence the aging time was fixed at 16 h for the rest of the study.

4.5. Solvent removal and drying

For all the samples in the present study, the solvent was distilled off maintaining a temperature of 100°C and the thick cake that resulted was subsequently dried in a laboratory oven at 120°C 16 h (conventional method) resulting in the formation of xerogels.

4.6. Calcination

It is reported by Schneider et al (**17**) that alumina prepared by SG method should be heated in inert gas or evacuated at high temperature prior to calcination (in air) to ensure removal of as much of the organic combustible moiety as possible. In the current work this was not followed since the samples were thoroughly dried for fairly long duration 16-24 h in a laboratory oven. All the dried samples in this study were calcined at 550 °C in a stream of air. Effect of calcinations temperature was studied over the range 500 to 600 °C. Results are given in Table 4.6

Depending on the aging duration (at sol stage) calcination was found to affect the final textural properties differently. Samples C-1 and C-2 differed in the following respect: C-1 was aged for 16 h as was the standard procedure in this work, where as sample C-2 was aged for 2h only. As seen from the results in Table 4.6, on calcinations sample C-1C shows an increase in both surface area as well as pore volume. Also the hysteresis loop form (Fig. 4.6,) clearly shows a transition from

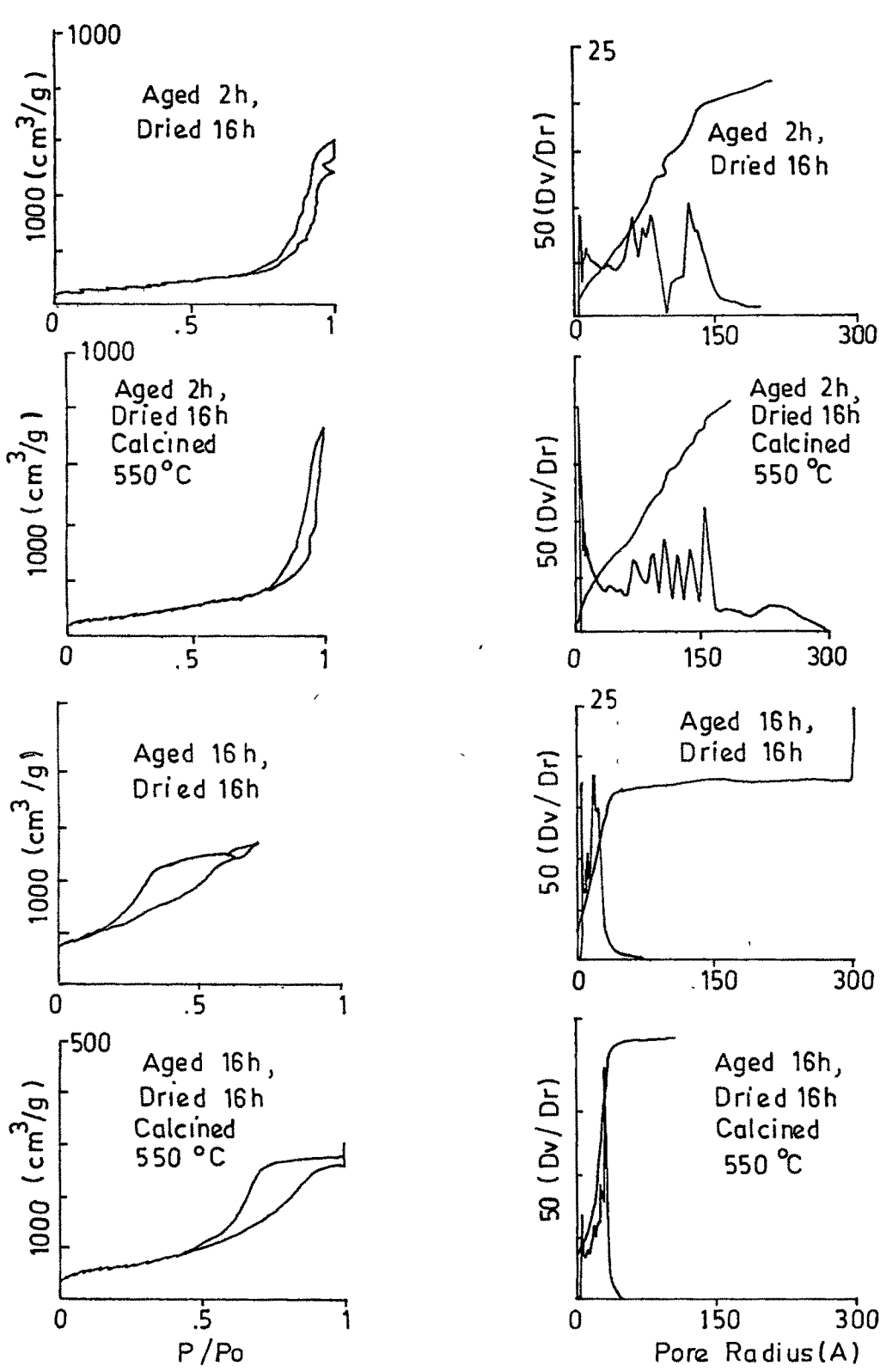


Figure 4.6(a): Effect of duration of drying on the textural properties : Hysteresis Loop Form

Figure 4.6(b): Effect of duration of drying on the textural properties : Pore size distribution curves

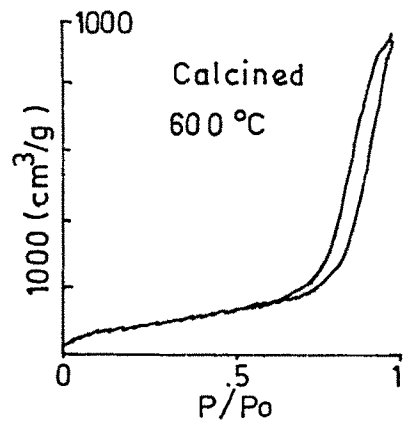
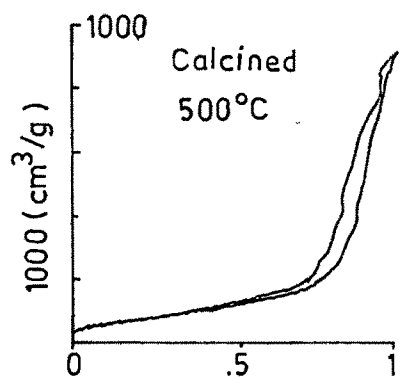
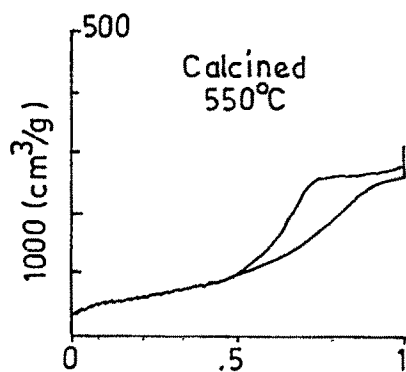


Figure 4.7(a) : Effect of calcination conditions on textural properties: Hysteresis Loop Form.

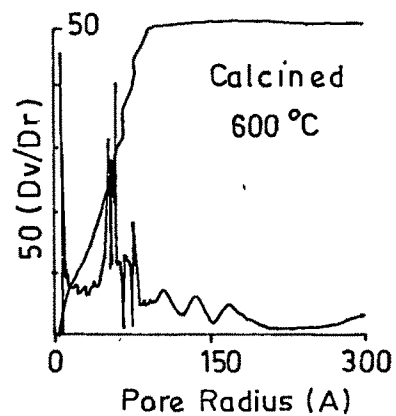
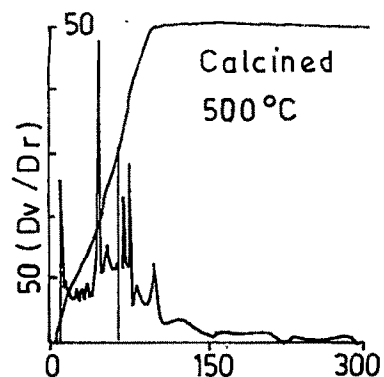
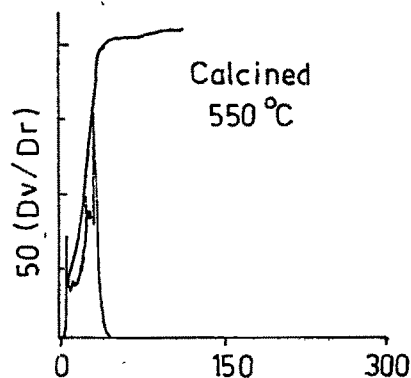


Figure 4.7(b) : Effect of calcination conditions on textural properties: Pore size distribution curves

type IV (with some traces of Type III) with some non-rigidity of structure (as evident from the sloping initial portion of the DBC) in the dried sample C-1D, to a mechanically rigid structure of type V with some traces of type IV. Sample C-2 on the other hand exhibits a decrease in both surface area and pore volume on calcinations. While there is no major change in the type of the HLF, transition from a non-rigid to rigid structure is evident from the transition of the initial DBC with a slope (in case of C-2D) to a flat plateau in the sample calcined at 550°C (sample C-2C). The difference in behaviour of these two samples is attributed to the poor consolidation of structure (densification) in case of sample C-2 due to the decreased aging duration at the sol stage.

Effect of calcinations temperature can be seen in the case of samples C-3-500 and C-3-600 calcined at 500°C and 600°C respectively (Fig. 4.7). Calcination at 500 or 600°C does not result in a gross difference in surface area or pore volume although the sample calcined at 600°C does show marginally higher surface area and better pore volume. Calcination temperature 550°C was maintained for the rest of the work.

4.7. Morphological Studies

Morphological studies were carried out using Scanning Electron Microscopy. The observations on these samples did not show any distinguishable differences in the morphology between dried and calcined samples. However, in the calcined samples with increasing pH, particle size has increased. The particle size was less than 0.5 microns at pH = 3 and it has increased to 2-3 microns at pH = 10. Similarly with solvent mixture ratio variations, a distinct change in the particle size is noticed as seen in figure 4.8.

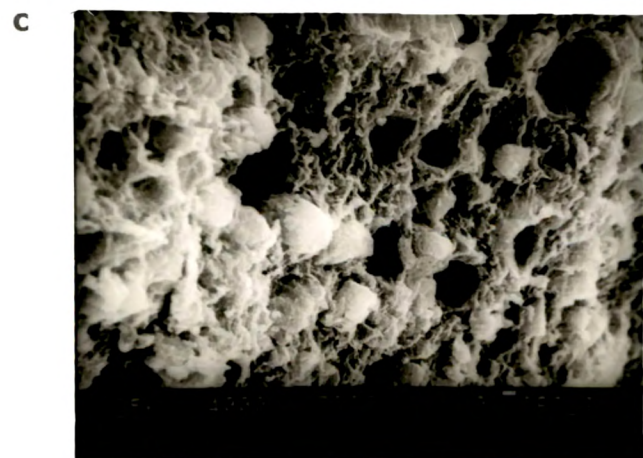


Figure 4.8a SEM Pictures of sol gel alumina prepared with pH (a) 3 (b) 7 (c) 10

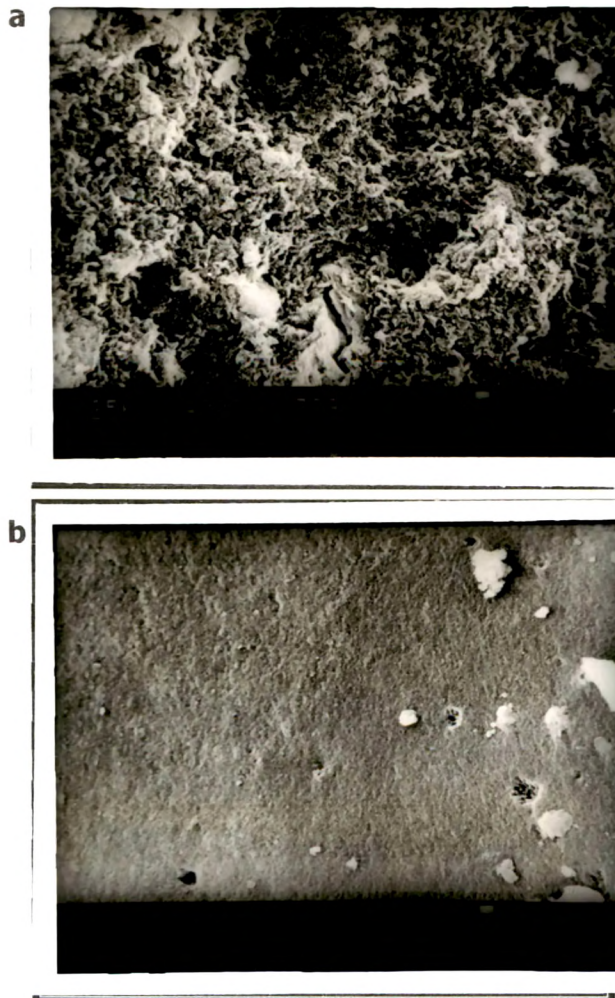


Figure 4.8b: SEM pictures of alumina prepared with (a) water to IPA ratio 10 ratio (b) water alone

Table 4.6: Effect of drying conditions and calcinations temperature on textural properties

Sample	Calcination	SA (m ² /g)	PV (ml/g)	Pore radius (Å) Max Contrib. (Distrbn.)	Hysteresis Loop Form*
C-1D (ageing – 16h)	120°C; 16h (Dried)	190	0.83	126-131 (Broad)	Type III or IV
C-1C	550°C 4h	255	1.09	156 (Broad)	Type IV or V
C-2D (ageing – 2h)	120°C; 16h (Dried)	256	0.59	18-29	Type I or II
C-2C	550°C 4h	226	0.44	22-35	Type I or II
C-3-500	500°C 4h	274	1.39	64-74	Type V
C-3-600	600°C 4h	290	1.48	53-77 (Rel. Broad)	Type V

4.8. 1 – Butene isomerization

The target reaction being catalytic dehydrogenation of n-decane, proper attenuation of acidity of the catalyst is critical from the point of view of both selectivity and stability. Formation of by-products viz. light olefins (through cracking) and aromatics require acidic sites. They adversely affect both selectivity as well as stability.

In general, crystalline aluminas are more acidic than amorphous aluminas. The alumina support prepared and used in the current study is of the latter type, selected, primarily on considerations of higher surface area and meso-porosity, which are favorable aspects for surface catalysis.

Isomerisation of 1-butene is a useful reaction in determining the type and strength of acidic sites on a catalyst (**18**). It is well documented in the literature that, at reactions temperatures above 300°C, double bond isomerisation is predominant, where as at temperatures below 300°C, it is the skeletal isomerisation that prevails.

Skeletal isomerisation is reported to be directly related to the fraction of strong Lewis acid sites.

The current study of 1-butene isomerisation was done at 350°C, atmospheric pressure, so as to enable assessment of the sites of both the above mentioned isomerisation reactions.

Relevant thermodynamic equilibrium data for the 1-butene-isomerisation reaction to relevant products are given below in Table 4.6. The Gibbs free energy of reaction was calculated from data published in API Tables (19). The values of ΔG_f^0 under the reaction conditions were determined by interpolation of data submitted to linear regression.

Table 4.6 Butene isomerisation results

CATALYST	1-C ₄ Conversion (%)	i-C ₄ Conversion (%)	Cis: Trans 2-C ₄
Al ₂ O ₃	63.6	0.64	0.78
SG-Al ₂ O ₃	33.7	0.7	1.07

The Solver routine in MS Excel XP was used for computing the fractional molar composition based on the equation $\Delta G_f = -RT \ln(K_{Eq})$;

Where δG_f = Free Energy of the relevant reaction Kcal/mole

R = The gas constant = 1.987×10^{-3} Kcal/deg/Mole

T = Reaction temperature in Kelvin

Constraints used were $\sum^I (C_i) = 1$; Where C_i is mole fraction of component I and $C_p/C_r = K_{Eq}$; Where C_r and C_p are mole fractions of reactant and products, assuming fugacity=1 for all components under the reaction conditions.

These studies reveal that Al₂O₃ prepared by the sol-gel route shows moderate activity for double bond isomerisation (w.r.t Cis: Trans 0.62 at thermodynamic equilibrium) but poor activity for skeletal isomerisation (54% at thermodynamic equilibrium). Hence the number of strong Lewis acid sites appears to be low.

4.9. Comparison of the characteristics of SG and OD alumina samples

For the sake of comparison, SG alumina prepared by hydrolysis of ASB at pH-9, H₂O/ASB =100 with 1:1 water: IPA as hydrolysant was used since maximum surface area, pore volume and mean pore radius, with predominantly meso porous structure could be obtained under these conditions. XRD patterns for SG and OD alumina samples are given in Fig.4. It is clearly seen that both are of gamma type

with SG alumina being highly amorphous. Textural properties of both alumina samples are given in Table 4.7

Table 4.7 Textural properties of SG and OD alumina

Property	SG alumina	OD alumina
Surface area m ² /g	379	160
Pore volume ml NTP/g	1.7	0.6
Mean Pore radius Å	103-106	85
Crystallite size Å	44	65
Crystallinity	Highly amorphous	Better crystallinity

To summarize, alumina samples with desired textural properties could be easily obtained by varying the preparation conditions/parameters via sol-gel process. With such an advantage, SG technique has become highly versatile process for preparation of tailor made supports/catalysts.

References

1. Keefer, in: *Silicon Based Polymer Science: A Comprehensive Resource*, eds. Zeigler, J.M. and Fearon, F.W.G., ACS Advances in Chemistry Ser. No. 224, (American Chemical Society: Washington, DC, 1990) pp. 227-240)
2. Prassas, M. and Hench, L.L., in: *Ultrastructure Processing of Ceramics, Glasses, and Composites*, eds. Hench, L.L. and Ulrich, D.R., (John Wiley and Sons: New York, 1984) pp. 100-125
3. JCPDS File number 29 - 1486
4. Bulent E. Yoldas, *Cer. Bull.*, **54**(3), p. 289, (1975)
5. Gomez et al, *Reaction Kinetics and Catalysis Letters*, **43**(2) 307-312 (1991)
6. Wefers, K. and Bell, FM, *Oxides and hydroxides of aluminium*, Technical paper no. 19, Aluminium Company of America, Pittsburgh, 1 – 51, (1972)
7. Wang, JA, Bokhimi, X., Morales, A., Novoro, O., Lopez, T. and Gomez, R., *J. Phys. Chem.*, **B103**, 299 – 303, (1999)
8. Sanchez, C. and Livage, J., *New J. Chem.*, **14**, 513 – 521, 1990
9. Brinker, C.J. *J. Non-Crystalline Solids*, **100**, 31-50, 1988
10. Engelhardt V.Q. et al. *Anorg. Allg. Chem.*, 1977, 418, 43.
11. An article from <http://www.psrc.usm.edu/mauritz/solgel.html> entitled "Sol - Gel Chemistry".
12. Poelz G., Riethmuller R., *Nucl. Instr and Methods*, **195**, p. 491, (1982)
13. Sanchez, C. and Livage, J., *New Journal of chem.*, **14**, p. 6, (1990)
14. Krishnan Balakrishnan, Richard D. Gonzalez, *J. of Catal.*, **144**, 395 – 413, (1993)

15. Salmones J., Garciafigueroa, E., Mayagoitia, V., Rojas, F. and Kornhauser, I., *Adsorption Science and Technology*, Vol. 15, No 9, 661 (1997)
16. Salmones, J., *Adsorption Science and Technology* **Vol. 15**, No 9, 1997
17. Schneider et al, *Catal. Rev., - Sci. Eng*, **37**(4), 515-556 (1995)
18. Zheng Xing Cheng and Vladimir Ponec, Selective Isomerisation of Butene to iso-butene, *J. Catal.*, **148**, 000-000, (1994)
19. American Petroleum Institute (API) Tables: Table 8p, monoolefins C₂ to C₅